

Synthesis and characterisation of novel metal-organic frameworks (MOFs) based on zirconium and bichinchonic acid

Noor Albayati^a, Waseem Yousif M. AL-dulaimy^b, Muhsin J Jweeg^c, Mohammed Kadhom^{d*}, Suhaib Salih^e and Ghassan Abdullah^e

^aDepartment of Science, College of Basic Education, University of Wasit, Azizia, Wasit, 52005, Iraq

^bDepartment of Chemistry, College of Science, University of Diyala, Baquba, Diyala, 32001, Iraq

^cCollege of Technical Engineering, Al-Farahidi University, Baghdad, 10070, Iraq

^dDepartment of Environment, College of Energy and Environmental Science, Al-Karkh University of Science, Baghdad 10081, Iraq

^eDepartment of Chemical Engineering, College of Engineering, Tikrit University, Saladin, 34001, Iraq

CHRONICLE

Article history:

Received March 25, 2023

Received in revised form

June 7, 2023

Accepted August 31, 2023

Available online

September 2, 2023

Keywords:

MOFs

Zr-Bads

Nanoparticles

Nanotechnology

Solvothermal

ABSTRACT

Metal-organic frameworks (MOFs) are a relatively new class of materials of unique porous structures and exceptional properties. Currently, more than 110,000 types of MOFs have been reported among the countless possibilities. In this study, we have synthesised a novel MOF using zirconium chloride as the metal source and 4,4'-dicarboxy-2,2'-biquinoline (bichinchonic acid disodium salt) as the linker, which reacted in N,N-Dimethylformamide (DMF) solvent. Three preparation methods were employed to prepare five types of the MOF, and they were compared to optimize the synthesis conditions. The resulting MOFs, named Zr-BADS, were characterised using scanning electron microscopy (SEM), energy dispersive spectroscopy (EDS), microscopy, and X-ray diffraction (XRD). By incorporating methanol into the preparation solvent, the surface area was increased to 396 m²/g. Additionally, the prepared MOFs exhibited amorphous shapes, with variations in size depending on the synthesis method. This research demonstrates the significance of the preparation method in controlling resulting particles' properties.

© 2024 by the authors; licensee Growing Science, Canada.

1. Introduction

Metal-organic frameworks (MOFs) are innovative materials that combine inorganic and organic components within a single hybrid structure. This type of porous material has garnered significant attention from scientists and engineers over the past few decades.¹ MOFs, first invented in the 1990s, are now recognized as crucial materials in various sectors and have been extensively studied in both fundamental and applied research.²

The self-assembly of metal ions or clusters as nodes and organic linkers as connections leads to the formation of MOFs, often exhibiting porosity in the micropore and mesopore ranges. MOFs possess numerous unique properties, with their remarkable surface area making them highly desirable for various applications, particularly gas storage.³ By 2020, it was reported that there were 500,000 predicted types of MOFs, with 90,000 already synthesised.⁴ Among the prepared MOFs, some have gained significant popularity and are produced in large quantities, such as UiO-66, while the utilization of others is still under investigation.⁵

In our research group, we have synthesized MOFs and employed them in various water treatment applications.^{6,7} MOFs have significantly enhanced the performance of reverse osmosis membranes compared to conventional additives.⁸ In fact,

* Corresponding author.

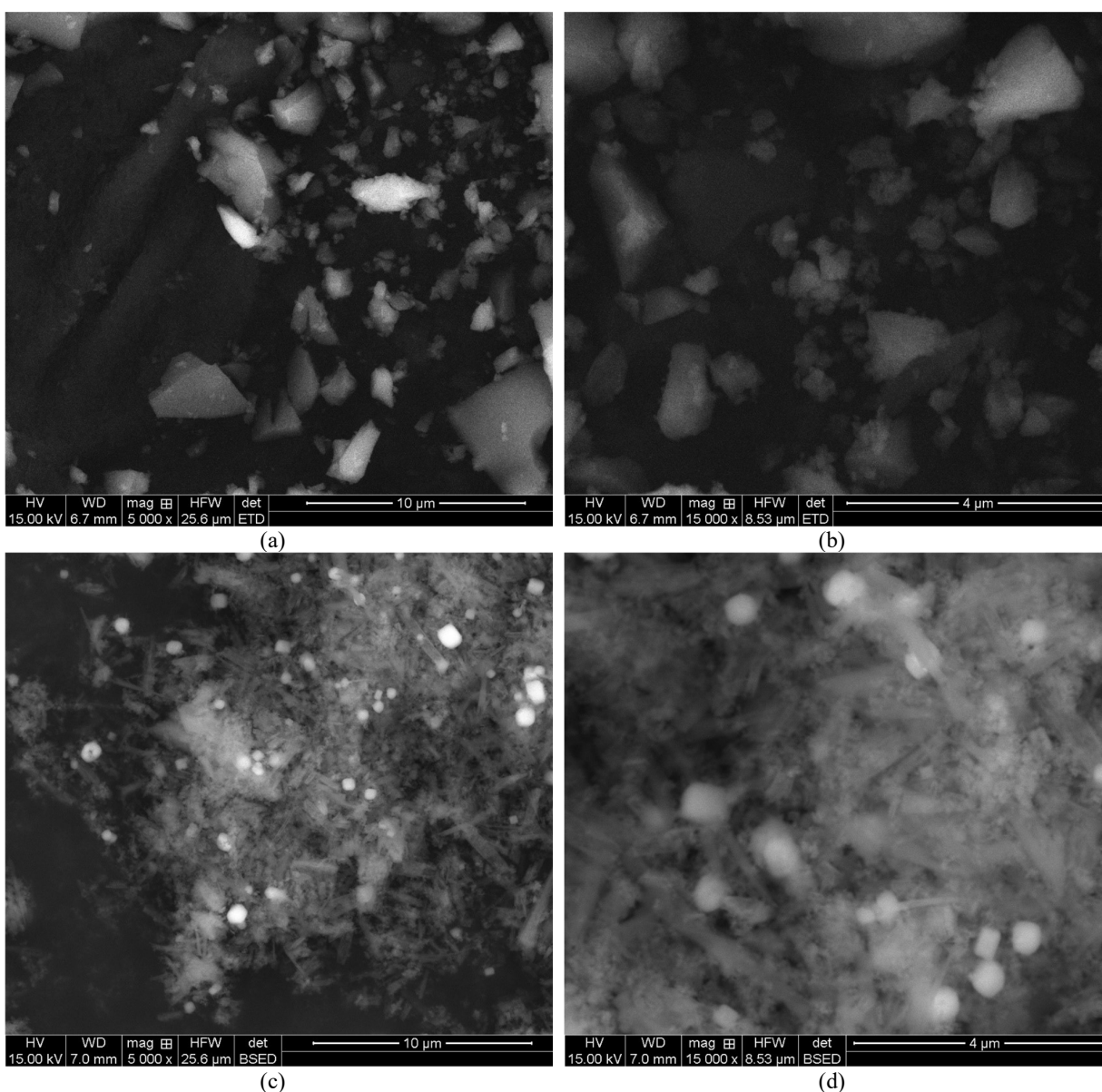
E-mail address kadhom@kus.edu.iq (M. Kadhom)

MOFs are applied in almost all types of applications, including the critical ones of drug delivery and medical treatments.⁹⁻¹² Consequently, our interest in developing suitable MOFs for environmental applications has grown. In this letter, we report on a novel zirconium-based MOF prepared under different conditions and characterized in terms of its nature, morphology, shape, size, and elemental analysis.

2. Results and Discussions

2.1 MOFs Morphology

The morphology of synthesized MOFs was examined using SEM to determine their geometric shapes and particle sizes. **Fig. 1** displays SEM images at scales of 10 μm and 4 μm for Zr-BADS-1 (a, b), Zr-BADS-2 (c, d), Zr-BADS-3 (e, f), Zr-BADS-4 (g, h), and Zr-BADS-5 (i, j), respectively. Analysis of the SEM images revealed that Zr-BADS-1 exhibited a size range of 300-1500 nm, whereas Zr-BADS-2 appeared to be smaller and more crystallized. This difference could be attributed to the solvent used, as DMF has high dissolving properties for both polar and non-polar compounds.¹³ Furthermore, observations indicated that Zr-BADS-3 displayed smaller particles compared to Zr-BADS-2. This variation could be attributed to the longer digestion time, despite using higher quantities of raw materials. Zr-BADS-4 was prepared by sonicating the mixture at room temperature for 30 minutes, resulting in SEM images showing relatively small particles of different sizes that were highly aggregated, forming a fuzzy cluster. On the other hand, Zr-BADS-5 exhibited larger particles compared to the other samples, which can be attributed to the simpler preparation conditions that omitted the thermal digestion step.



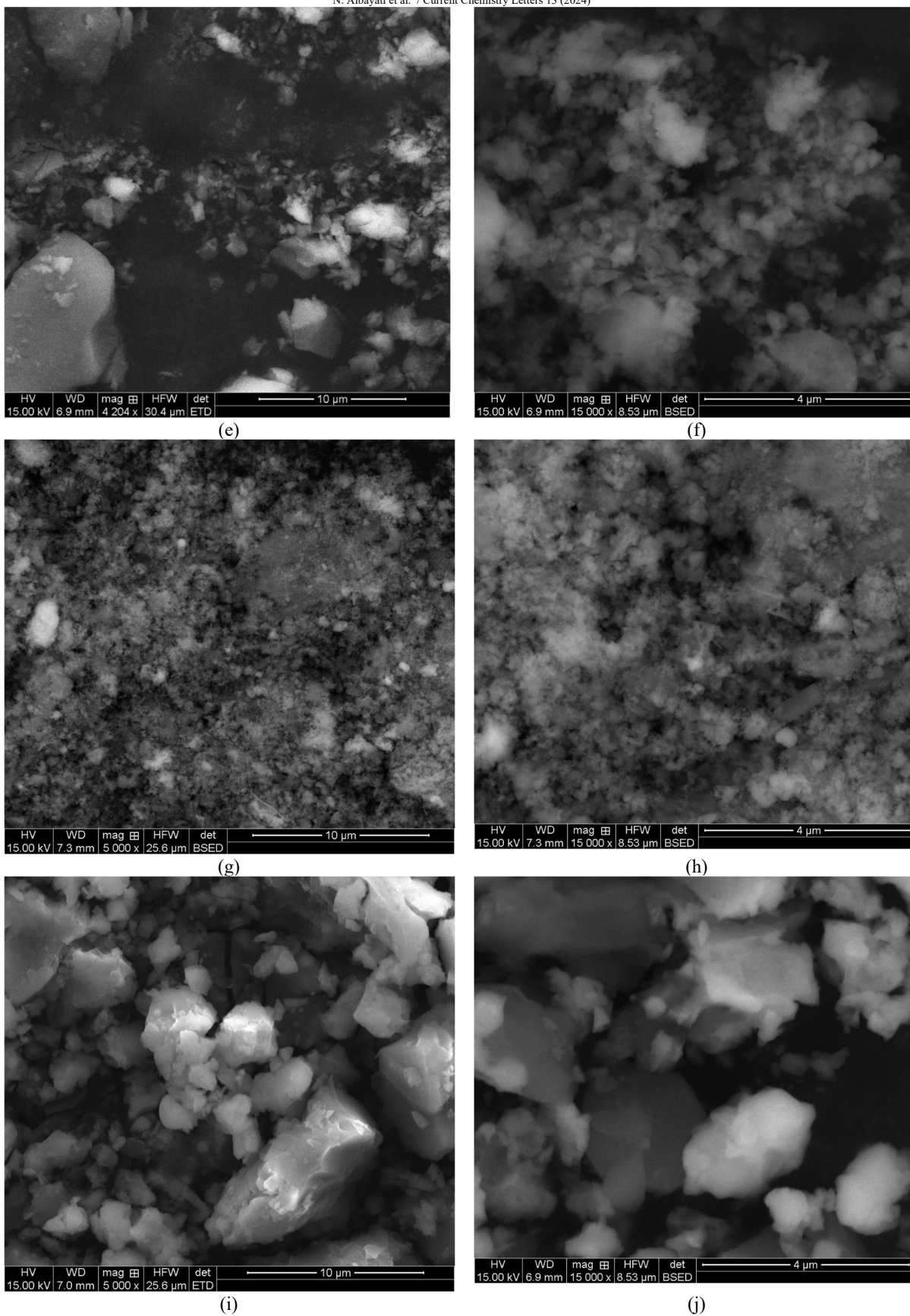
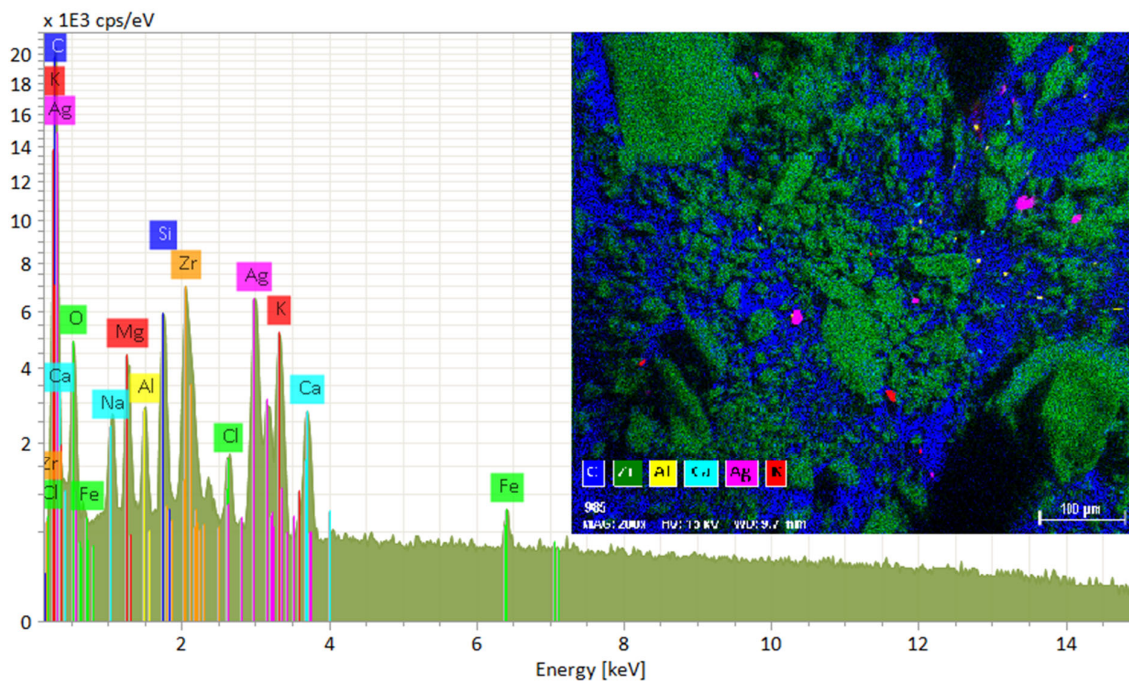


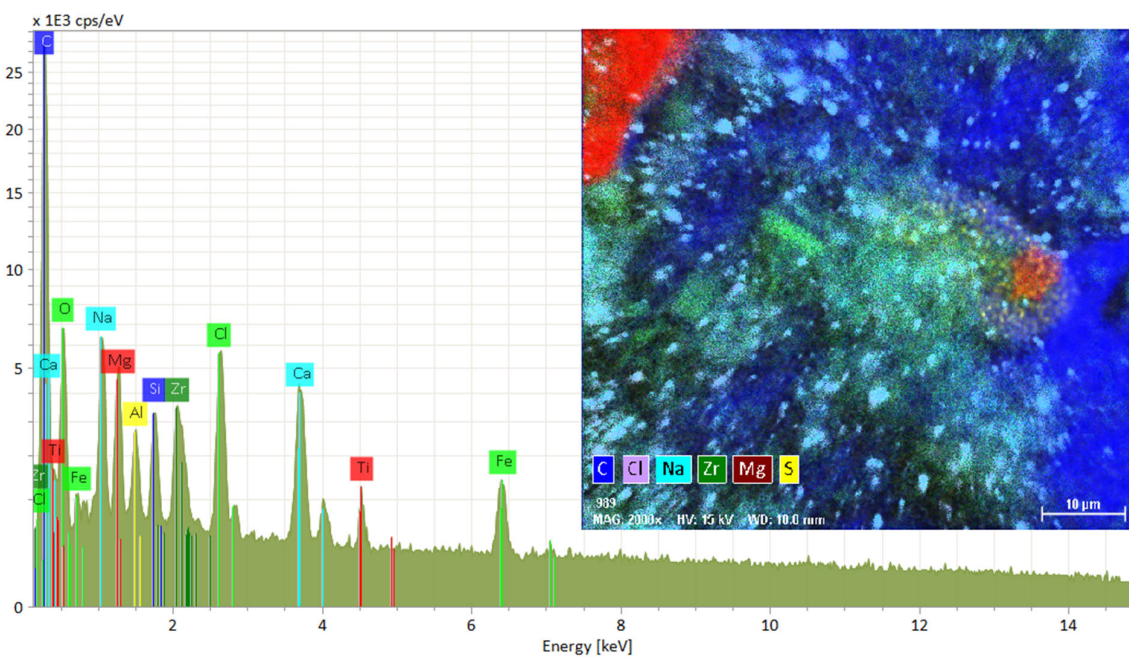
Fig. 1. SEM images of scales 10 μm and 4 μm of Zr-BADS-1 a and b, Zr-BADS-2 c and d, Zr-BADS-3 e and f, Zr-BADS-4 g and h, and Zr-BADS-5 i and j, respectively.

2-2 EDS Analysis

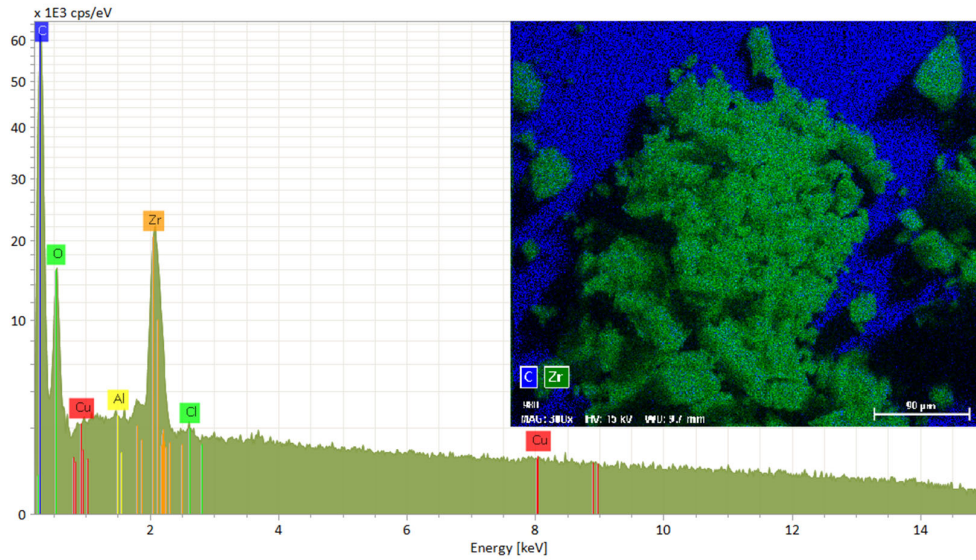
Fig. 2 depicts the EDS analysis, peak distribution, and identification images for (a) Zr-BADS-1, (b) Zr-BADS-2, (c) Zr-BADS-3, (d) Zr-BADS-4, and (e) Zr-BADS-5. The images reveal that the carbon background from the sticky holder piece appears blue, while the particles appear green due to the predominant presence of zirconium. The distribution of metals varies among the different samples, with Zr-BADS-2 exhibiting the most optimal metallic mixture, confirming the formation of the MOF. In terms of chemical peaks, Zr-BADS-1 and Zr-BADS-2 exhibit a greater number compared to the other samples, as they underwent the commonly used solvothermal synthesis process. Despite the simplicity of the preparation method and the larger particle size observed in Zr-BADS-5, satisfactory elemental distribution is observed. To determine the particle shapes, a microscope examination was conducted as shown in **Fig. S1**.



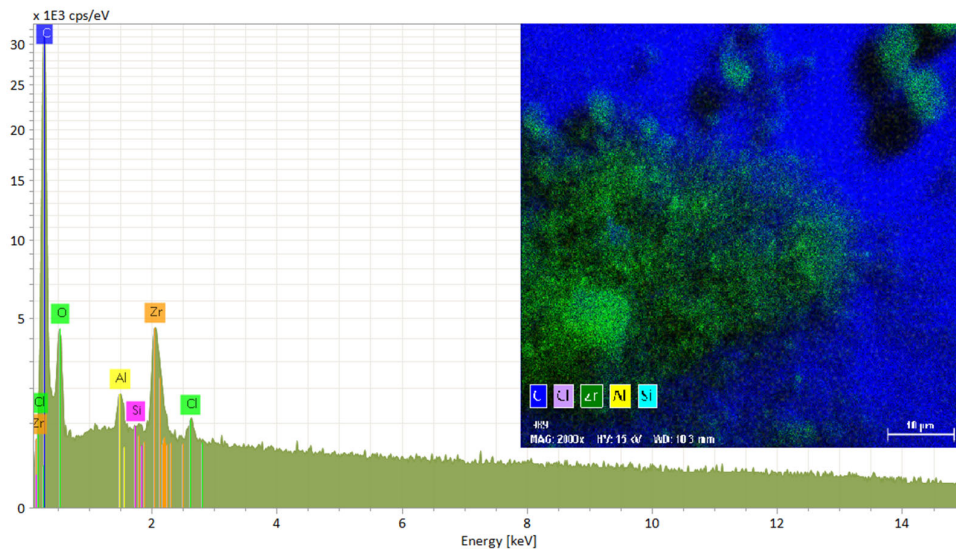
(a)



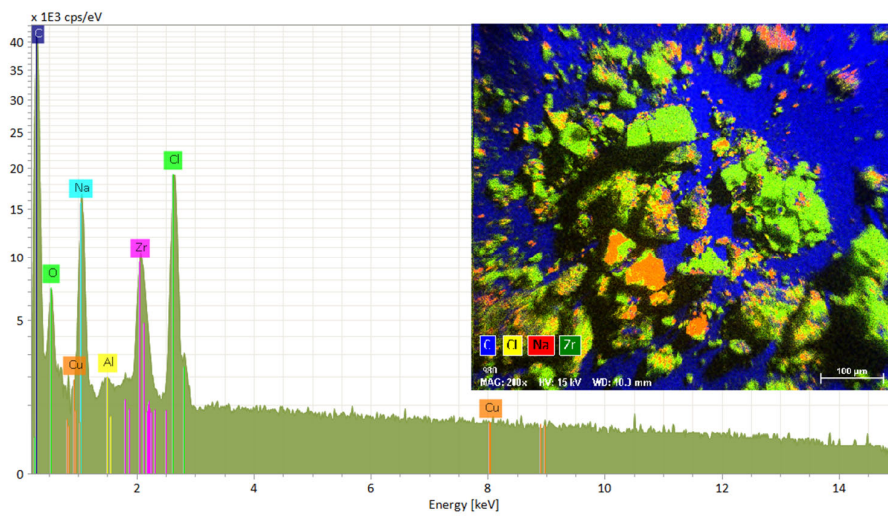
(b)



(c)



(d)



(e)

Fig. 2. EDS analysis for (a) Zr-BADS-1, (b) Zr-BADS-2, (c) Zr-BADS-3, (d) Zr-BADS-4, and (e) Zr-BADS-5.

2.3 BET Analysis

Different surface area values were obtained for the Zr-BADS MOFs. Among them, Zr-BADS-1 exhibited the highest surface area, which can be attributed to the inclusion of 10% methanol in the solvent during its preparation. The surface area of the MOF is influenced by factors such as the properties and volatility of the solvent.¹⁴ Additionally, other conditions such as temperature and reaction time can also impact the final specifications of the product. The surface areas of Zr-BADS-1, -2, -3, -4, and -5 were measured as 396.1, 354.3, 293.7, 137.4, and 99.7 m²/g, respectively.

2.4 XRD analysis

X-ray diffraction (XRD) is a commonly used technique to characterize the crystal structure of materials and provide information about their structural properties.¹⁵ The XRD test for Zr-BADS-1 is shown in **Fig. 3**, where four peaks appear. The highest peaks are detected at 39.5° and 44.5°; The mean crystal dimension (D) was determined using Scherrer's equation with the peak observed at 39.5° and it was 17.6 nm. This value is lower than the commonly reported Zr-based MOF UiO-66 which shows less crystallinity.¹⁶

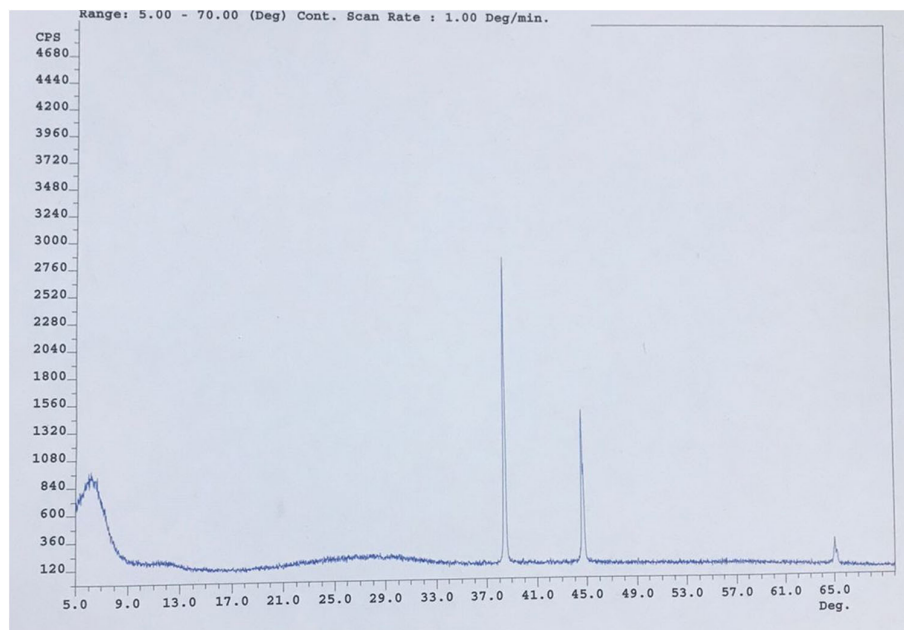


Fig. 3. XRD analysis for Zr-BADS-1

3. Conclusion

In this study, a new MOF named Zr-BADS was synthesized by reacting ZrCl₄ and BADS. Three different preparation methods were employed to obtain five types of Zr-BADS, and their properties were compared. Interestingly, regardless of the preparation method, all the resulting Zr-BADS products exhibited a yellow color and demonstrated a high surface area, indicating their potential for various applications. It is important to note that we also investigated the application of Zr-BADS in water treatment, and we obtained promising results, which will be reported soon.

Acknowledgment

The authors would like to thank Prof. Baolin Deng for partially supporting this work. Also, we are grateful for the EM core at the University of Missouri-Columbia for their help to obtain the EDS analysis.

4. Material and Methods

4.1 Chemicals

To prepare the MOF, we obtained the following chemicals from Sigma-Aldrich (St. Louis, MO, USA): 4,4'-dicarboxy-2,2'-biquinoline ((bichinchonic acid) disodium salt) (BADS) (C₂₀H₁₀N₂O₄Na₂) with a water content of 2.5 mol/mol and a molecular weight of 388.3, zirconium (IV) chloride (ZrCl₄) with a purity of 99.5%, dimethylformamide (DMF) with a purity of 99.9%, and methanol with a minimum purity of 99%. For cleaning and other purposes, we utilized water supplied by the Synergy185 Millipore DI water system (18.2 MΩ-cm, EMD Millipore Corp., Billerica, MA, USA).

4.2 MOF Preparation

The new MOF, named Zr-BADS, was prepared using zirconium chloride (ZrCl_4) as the source of the metallic component and 4,4'-dicarboxy-2,2'-biquinoline ((bicinchoninic acid) disodium salt) as the linker in a DMF medium. The preparation details are provided in **Table 1**, where three different methods were employed: solvothermal, sonication, and simple. In the solvothermal method, the mixture was combined in a 500 ml Teflon liner and sealed within a metal autoclave. For this study, three samples, denoted as Zr-BADS-1, -2, and -3, were prepared using this method. The mixture was then placed in a furnace and maintained at 120 °C for a specified duration. Subsequently, the autoclave was removed from the furnace and allowed to cool down to room temperature (RT). The resulting product was separated using centrifugation. The product was then washed three times with methanol and centrifuged to remove any remaining DMF and residual raw materials. Finally, the product was dried overnight at 80 °C in an oven.

For the Zr-BADS-4 sample, the mixture was subjected to sonication for 30 minutes at RT. The sonication method appears to be the fastest preparation method compared with others. In this method, the raw materials (ratios are illustrated in **Table 1**) the salt was set in a vial and the solvent was added to it. Then, the linker was added to the mixture and set in the sonicator for a certain time. Sonochemistry, positioned at the intersection of physics and chemistry, investigates the influence of ultrasonic waves on the surrounding medium. Notably, the chemical outcomes stemming from ultrasound irradiation arise not from direct acoustic wave interactions at the atomic and microscopic scales, but rather from the occurrence of acoustic cavitation—a phenomenon induced by ultrasonic irradiation within the liquid system.¹⁷

On the other hand, for Zr-BADS-5, the mixture was placed in a dish and dried using airflow at RT. Zr-BADS-4 and -5 samples underwent the same purification and drying procedures as of the solvothermal method. One general observation is that the MOFs are prepared directly, and upon adding the raw materials (both of which are white), they undergo an immediate reaction and turn yellow in color. The expected synthesis reaction and structure of the prepared MOF are presented in **Fig. 4**.

Table 1. Preparation conditions of Zr-BADS

Sample name	Components ratios (metal: linker: solvent)	Time (h)	Temperature (°C)	Notes
Zr-BADS-1	1: 1: 500	48	120	Prepared by solvothermal process: The solvent contained 10% methanol
Zr-BADS-2	0.25: 0.25: 500	48	120	Prepared by solvothermal process
Zr-BADS-3	1: 1: 500	72	120	Prepared by solvothermal process
Zr-BADS-4	1: 1: 500	0.5	RT	Prepared by sonication process
Zr-BADS-5	1: 1: 500	5	RT	Dried by blowing air

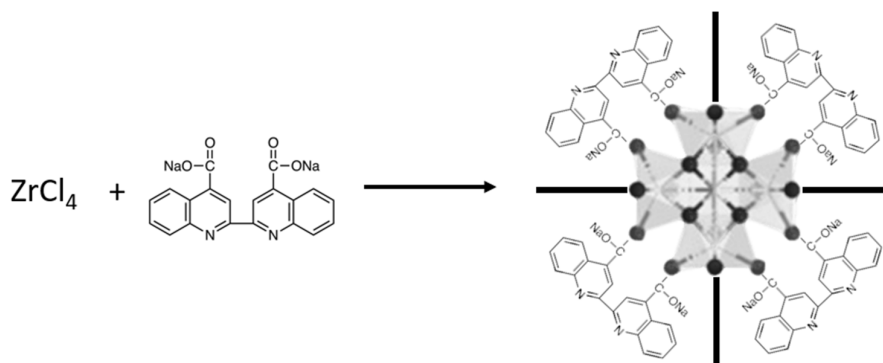


Fig. 4. Zr-BADS preparation reaction

4.3 Characterization Methods

The shape and size of the Zr-BADS MOF particles were evaluated using an SEM device, specifically the FEI Quanta 600F Environmental SEM. To prepare the samples for SEM analysis, Zr-BADS particles were dispersed onto a carbon tape that was affixed to a stage. Subsequently, a platinum coating was applied using a sputter coater (K575x, Emitech, Kent, UK) under operating conditions of 20 mA for 1 minute. Notably, the SEM device was equipped with a Bruker EDS system, allowing for elemental analysis of the samples. To measure the surface area of the MOF, a Beckman Coulter SA 3100 analyzer was employed, following the principles of the Brunauer–Emmett–Teller (BET) theory. The surface area measurement was conducted at a temperature of 120 °C. Prior to the analysis, the sample was degassed at 120 °C to eliminate any potential moisture. The Brunauer–Emmett–Teller method was then employed to calculate the surface area. The XRD data were collected within the 2θ range of 5–65° at a scanning rate of 1° per minute, utilizing a Bruker D8 diffractometer equipped with a Cu- $K\alpha$ ($\lambda = 0.15406$ nm) radiation source.

References

- 1 Jodłowski P. J., Dymek K., Kurowski G., Hyjek K., Boguszewska-Czubara A., Budzyńska B., Pajdak A., Kuterasiński Ł., Piskorz W., Jeleń P., Sitarz, M. (2023) In vivo and in vitro studies of efficient mephedrone adsorption over zirconium-based metal-organic frameworks corroborated by DFT+D modeling. *Microporous Mesoporous Mater.*, 359 112647. (DOI: 10.1016/j.micromeso.2023.112647).
- 2 Jodłowski P. J., Kurowski G., Dymek K., Oszejca M., Piskorz W., Hyje K., Wach A., Pajdak A., Mazur M., Rainer D. N., Wierzbicki D., Jeleń P., Sitarz M. (2023) From crystal phase mixture to pure metal-organic frameworks – Tuning pore and structure properties. *Ultrason. Sonochem.*, 95 106377. (DOI: 10.1016/j.ultsonch.2023.106377).
- 3 Jones C. W. (2022) Metal–Organic Frameworks and Covalent Organic Frameworks: Emerging Advances and Applications. *JACS Au*, 2 1504–1505. (DOI:10.1021/jacsau.2c00376).
- 4 Moosavi S. M., Nandy A., Jablonka K. M., Ongari D., Janet J. P., Boyd P. G., Lee Y., Smit B., Kulik H. J. (2020) Understanding the diversity of the metal-organic framework ecosystem. *Nat. Commun.*, 11 4068. (DOI: 10.1038/s41467-020-17755-8).
- 5 Kadhom M., Al-Furajji M., Salih S., Al-Obaidi M.A., Abdullah G.H., Albayati, N. (2023) A review on UiO-66 applications in membrane-based water treatment processes. *J. Water Process Eng.*, 51 103402. (DOI: 10.1016/j.jwpe.2022.103402).
- 6 Sohrabi H., Maleki F., Khaaki P., Kadhom M., Kudaibergenov N., Khataee A. (2023) Electrochemical-Based Sensing Platforms for Detection of Glucose and H₂O₂ by Porous Metal–Organic Frameworks: A Review of Status and Prospects. *Biosensors*, 13 347. (DOI: 10.3390/bios13030347).
- 7 Kadhom M., Deng, B. (2018) Metal-organic frameworks (MOFs) in water filtration membranes for desalination and other applications. *Appl. Mater. Today*, 11 219–230. (DOI: 10.1016/j.apmt.2018.02.008).
- 8 Kadhom M., Hu W., Deng, B. (2017) Thin film nanocomposite membrane filled with metal-organic frameworks UiO-66 and MIL-125 nanoparticles for water desalination. *Membranes*, 7 7020031. (DOI: 10.3390/membranes7020031).
- 9 Hyjek K., Jodłowski, P. (2023) Metal-organic frameworks for efficient drug adsorption and delivery. *Sci. Radices.*, 2 (2) 118-189. (DOI: 10.58332/scirad2023v2i2a03).
- 10 Dymek K., Kurowski G., Kuterasiński Ł., Jędrzejczyk R., Szumera M., Sitarz M., Pajdak A., Kurach Ł., Boguszewska-Czubara A., Jodłowski, P. J. (2021) In Search of Effective UiO-66 Metal–Organic Frameworks for Artificial Kidney Application. *ACS Appl. Mater. Interfaces*, 13 (38) 45149–45160. (DOI: 10.1021/acsmi.1c10732).
- 11 Jodłowski P. J., Kurowski G., Kuterasiński Ł., Sitarz M., Jeleń P., Jaśkowska J., Kołodziej A., Pajdak A., Majka Z., Boguszewska-Czubara, A. (2021) The Application of Defective UiO-66 Metal–Organic Framework Materials to Prevent the Onset of Heart Defects—In Vivo and In Vitro. *ACS Appl. Mater. Interfaces*, 13 (1) 312–323. (DOI: 10.1021/acsmi.1c10732).
- 12 Jodłowski P. J., Dymek K., Kurowski G., Jaśkowska J., Bury W., Pander M., Wnorowska S., Targowska-Duda K., Piskorz W., Wnorowski A., Boguszewska-Czubara, A. (2022) Zirconium-Based Metal–Organic Frameworks as Acriflavine Cargos in the Battle against Coronaviruses—A Theoretical and Experimental Approach. *ACS Appl. Mater. Interfaces*, 14 (25) 28615–28627. (DOI: 10.1021/acsmi.1c10732).
- 13 Phadagi R., Singh S., Hashemi H., Kaya S., Venkatesu P., Ramjugernath D., Ebenso E. E., Bahadur I. (2021) Understanding the role of Dimethylformamide as co-solvents in the dissolution of cellulose in ionic liquids: Experimental and theoretical approach. *J Mol. Liq.*, 328 115392. (DOI: 10.1016/j.molliq.2021.115392).
- 14 Albayati N., Kadhom M. (2020) Preparation of functionalised UiO-66 metal–organic frameworks (MOFs) nanoparticles using deep eutectic solvents as a benign medium. *Micro Nano Lett.*, 15 1075–1078. (DOI: 10.1049/mnl.2020.0360).
- 15 Luan Y., Qi Y., Gao H., Andriamitantoa R. S., Zheng N., Wang G. (2015) A general post-synthetic modification approach of amino-tagged metal–organic frameworks to access efficient catalysts for the Knoevenagel condensation reaction. *J. Mater. Chem. A*, 3 17320. (DOI: 10.1039/c5ta00816f).
- 16 Wang Y. L., Zhang S., Zhao Y. F., Bedia J., Rodriguez J. J., Belver C. (2021) UiO-66-based metal organic frameworks for the photodegradation of acetaminophen under simulated solar irradiation. *J. Environ. Chem. Eng.*, 9 (5) 106087. (DOI: 10.1016/j.jece.2021.106087).
- 17 Kim H. N., Suslick K. S. (2018) The Effects of Ultrasound on Crystals: Sonocrystallization and Sonofragmentation. *Crystals*, 8 (7) 280. (DOI: 10.3390/cryst8070280).

